

## POSSIBLE CONSTRAINTS ON EARLY MARS ATMOSPHERIC PRESSURE FROM SMALL ANCIENT CRATERS.

Edwin Kite (ekite@caltech.edu)<sup>1</sup>, Jean-Pierre Williams<sup>2</sup>, Antoine Lucas<sup>1</sup>, and Oded Aharonson<sup>1,3</sup>. <sup>1</sup>Caltech; <sup>2</sup>UCLA;

<sup>3</sup>Weizmann Institute of Science, Helen Kimmel Center for Planetary Science.

**Summary:** The single most important control on long-term climate change on Mars is thought to be decay of the CO<sub>2</sub>-dominated atmosphere, but direct constraints on paleoatmospheric pressure  $P$  are few<sup>1</sup>. Of particular interest is the climate that allowed rivers to flow early in Mars history, which was affected by  $P$  via direct and indirect greenhouse effects<sup>2-6</sup>. The size of craters embedded within ancient layered sediments is a proxy for  $P$ : the smaller the minimum-sized craters that form, the thinner the past atmosphere<sup>7-9</sup>. We used HiRISE images and Digital Terrain Models (DTMs) to identify ancient craters among the river deposits of Aeolis<sup>10</sup> close to Gale crater, and compared their sizes to models of atmospheric filtering of impactors by thicker atmospheres<sup>11-12</sup>. We obtain an upper limit of  $P \leq 760 \pm 70$  mbar, rising to  $P \leq 1640 \pm 180$  mbar if rimmed circular mesas are excluded. Our work assumes target properties appropriate for desert alluvium<sup>13</sup>: if sediment developed bedrock-like rock-mass strength by early diagenesis, the upper limit is greatly increased. If Mars did not have a stable multibar atmosphere at the time that the rivers were flowing, the warm-wet CO<sub>2</sub> greenhouse of Ref. 2 is ruled out. Our paper on this topic is in review; the preprint is <http://arxiv.org/abs/1304.4043>

**Introduction:** Planetary atmospheres brake, ablate, and fragment small asteroids and comets, filtering out small hypervelocity surface impacts and causing fireballs, airbursts, meteors, and meteorites. “Zap pits” as small as 30  $\mu\text{m}$  are known from the airless Moon, but small craters are depleted on Mars, Earth, Titan and Venus below diameters that increase with atmospheric thickness<sup>7-9</sup>.

Contrary to early work<sup>2</sup>, it is doubtful that increasing CO<sub>2</sub> pressure ( $\approx$ total atmospheric pressure,  $P$ ) is enough to raise early Mars mean-annual surface temperature ( $T_{av}$ ) to the freezing point<sup>5</sup>. However, increased CO<sub>2</sub> aids transient surface liquid water production by impacts, volcanism, or infrequent orbital conditions<sup>3-4,6</sup>. Existing data requires an early epoch of massive atmospheric loss to space; suggests that the present-day rate of escape to space is small; and offers evidence for only limited carbonate formation<sup>14</sup>. These data have not led to convergence among atmosphere evolution models, which must balance poorly understood fluxes from volcanic degassing, escape to space, weathering, and photolysis<sup>16</sup>. More direct measurements<sup>17</sup> are required to determine the history of Mars’ atmosphere, and the size of exhumed ancient craters has been previously suggested as a paleo- $P$  proxy (e.g., Ref 17).

Here we obtain a new upper limit on early Mars atmospheric pressure from the size-frequency distribution of small ancient craters interspersed with river deposits in Aeolis, and simulations of the effect of  $P$  on the crater flux. The craters are interbedded with river deposits with inferred peak discharge  $10^1$ - $10^3$  m<sup>3</sup>/s (Ref. 10). Therefore, the atmospheric state they record corresponds to an interval of time when Mars was substantially wetter than the present, probably  $> 3.7$  Ga.

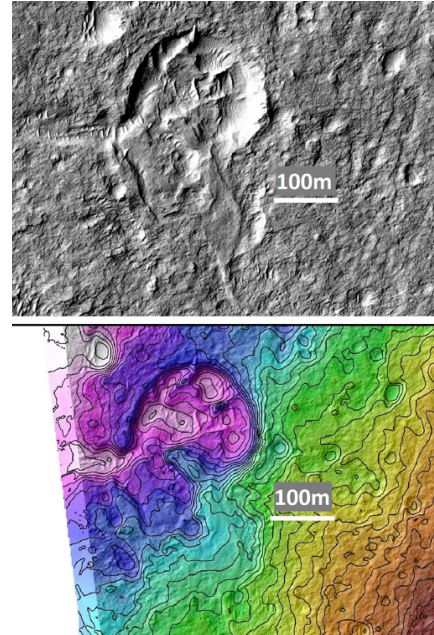


**Fig. 1.** Example of an embedded crater. Top: Crater partly exhumed from beneath fluvial channel deposit. 238 m diameter. ESP\_019104\_1740. Bottom: Same crater, with 1m DTM contours.

**Data:** Aeolis Dorsa’s stratigraphy is shot through with the deposits of large rivers, and when these overlie a crater, that crater must be as ancient as the rivers<sup>18</sup> (Fig. 1). We built 2 HiRISE DTMs/orthophotos (areas of ESP\_019104\_1740 and PSP\_07474\_1745), and classified craters as definite ancient craters (visibly embedded within stratigraphy: e.g., overlain by river deposit) ( $n = 56$ , median diameter  $D_{50} = 107$  m, 10<sup>th</sup>-percentile diameter  $D_{10} = 50$  m), rimmed circular mesas (RCM) ( $n = 71$ ,  $D_{50} = 48$  m,  $D_{10} = 21$  m), or candidate ancient crater ( $n = 192$ ,  $D_{50}$  also 48 m,  $D_{10}$  also 21 m; candidates are not considered further, but their inclusion would strengthen our conclusions). We measured  $D$  by fitting circles to preserved edges/rims. RCM appear as disks in raw HiRISE images. We interpret them as the erosion-resistant fills/floors of impact craters that were topographically inverted during the deflation of the target unit. We plot them separately, but consider them to be probable ancient craters.

**Model:** We generated synthetic crater populations for varying  $P$  (ref. 11) by drawing randomly from the size distribution of Ref. 22 and the initial-velocity distribution of Ref. 23. Compositions, densities and ablation coefficients follow Ref. 24. The approach is conceptually similar to that of previous studies<sup>12</sup>, and benefits from measurements of the current Martian cratering flux<sup>26</sup>. The atmosphere drains kinetic energy from impactors via drag and ablation. Fragmentation occurs when ram pressure exceeds  $M_{str}$ , disruption strength. Our conclusions are insensitive to  $M_{str}$  variations within the range reported for Earth fireballs<sup>24</sup>.  $M_{str}$  adjusted to match Ref. 26’s observed

Mars disrupted-impactor fraction falls within the Earth fireball range. Particles braked to  $<500$  m/s would not form hypervelocity craters and are removed from the simulation. Crater sizes are calculated using  $\pi$ -group scaling<sup>20</sup>. We apply a geometric correction for exhumation from a cratered volume, and correct  $P$  for the ( $\sim 2$ km) elevation of our DTMs. We do not track secondaries; meter-sized endoatmospheric secondaries are likely to be braked to sub-hypervelocity speeds for the relatively thick atmospheres we are evaluating. In other words, if wet-era small craters are secondaries, then early Mars' atmosphere was thin. A caveat is that impacts transiently modify local  $P$ .

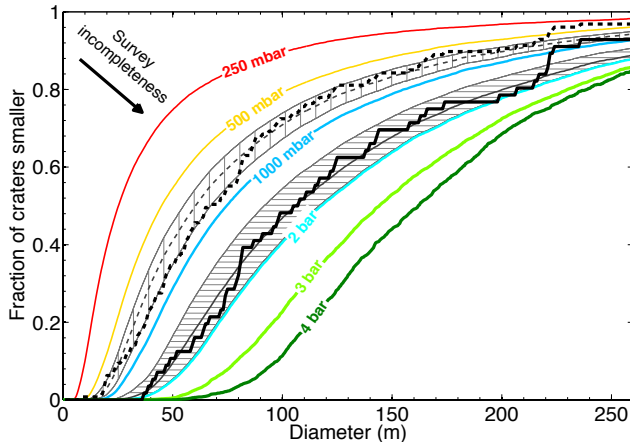


**Fig. 2.** Comparison of model crater size-frequency distributions to observations. Solid black line corresponds to definite embedded craters. Dashed black line additionally includes RCMs. Colored lines show model predictions for atmospheric filtering of small impactors. Gray hatched regions correspond to  $2\sigma$  statistical-error envelope around the best-fit paleopressure to the data (best fit shown by thick gray lines). Survey incompleteness leads to overestimates of median crater size; best fits are upper limits.

**Paleopressure constraint:** We compared the model to the combined dataset (Fig. 2). Combined best fits are  $P = 1640 \pm 180$  mbar, falling to  $P = 760 \pm 70$  mbar if RCM (candidate syndepositional impact craters) are also included (Fig. 2). Better preservation could allow still smaller embedded craters to be uncovered, so these are upper limits.

Results are sensitive to target strength, as expected<sup>19</sup>. Increasing target rock-mass strength to a hard-rock-like 6.9 MPa (ref. 20) increases the combined upper limit on  $P$  to  $\sim 1.8$  bars. Our work assumes weak soil-like target strength appropriate for river alluvium in an aggrading sedimentary deposit: if sediment developed bedrock-like rock-mass strength by early diagenesis, the upper limit is greatly increased. Sensitivity tests show a relatively minor effect of fragmentation on the results.

**Environmental interpretation:** Our technique rules out a thick *stable* paleoatmosphere, not atmospheric collapse-reinflation cycles on orbital timescales. General Circulation Model (GCMs) predict that atmospheric collapse to form  $\text{CO}_2$ -ice sheets and subsequent reinflation might be triggered by obliquity change (e.g., ref. 5). In principle our DTMs could integrate over  $\sim 10^6$ - $10^8$  years of sedimentation<sup>18</sup> (many collapse-and-reinflation cycles). Therefore one interpretation is

that smaller ancient craters formed while the atmosphere was collapsed, while rivers formed during high-obliquity, thick-atmosphere intervals. However, published models indicate that collapse to form polar  $\text{CO}_2$ -ice sheets only occurs for pressures less than our upper limit<sup>5</sup>.

Revisions to  $\text{CO}_2$ 's infrared opacity indicate that *any* amount of  $\text{CO}_2$  is insufficient to warm early Mars *Tav* to the freezing point<sup>5</sup>. Even if further work incorporating radiatively-active clouds moderates this conclusion, our result is an independent constraint on stable  $\text{CO}_2/\text{H}_2\text{O}$  warm-wet solutions (Figure 3). Increased  $\text{CO}_2$  below the warm-wet threshold does prime Mars climate for surface liquid water production by other relatively short-lived mechanisms, by adding to the greenhouse effect, pressure-broadening the absorption lines of other gases<sup>4</sup>, suppressing evaporitic cooling<sup>6</sup>, and increasing atmospheric heat capacity<sup>3</sup>.

**Synthesis:** Isotopes suggest that  $>90\%$  of initial atmosphere was lost  $>4.1$  Ga. Subsequent loss rates are less clear. The MAVEN orbiter will measure modern loss processes. Ref. 16 infers  $P > 120$  mbar from the terminal velocity of a bomb sag in Gusev crater, consistent with our result. Our result is consistent with other studies (e.g., Refs. 21, 25), which generally require more assumptions than our method. Future work could test the 40-year-old prediction of a connection between drying and atmospheric decay by applying the small-crater technique to sedimentary deposits of different ages. This could yield a time series of constraints on  $P$ , stratigraphically coordinated to the sedimentary record of Mars' great drying.

**Acknowledgements:** We thank I. Daubar, J. Dufek, B. Ehlmann, W. Fischer, M. Kahre, I. Halevy, K. Lewis, M. Manga, R. Ramirez, M. Rice, and A. Soto for discussions.

**References:** [1] Beatty, D.W., et al., *Astrobiology* 5, 663-689 (2005). [2] Pollack, J.B., et al., *Icarus* 71, 203-224 (1987). [3] Segura, T.L., et al., *JGR* 113, E11007 (2008). [4] Tian, F., et al., *EPSL* 295, 412-418 (2010). [5] Forget, F., et al., *Icarus* 222, 81-99 (2013). [6] Kite, E.S., Halevy, I., Kahre, M.A., Wolff, M.J., Manga, M., *Icarus* 223, 181-210 (2013). [7] Chappelow, J.E., & Golombek, M.P., *JGR* 115, E00F07 (2010). [8] Wood, C.A., et al., *Icarus* 206, 344-344 (2010). [9] Venus Crater Database v.3; R.R. Herrick <http://www.lpi.usra.edu/resources/vc/> [10] Burr, D.M., et al., *JGR* 115, E07011 (2010). [11] Williams, J.-P., et al., EPSC abstracts, vol 7, EPSC2012-95 (2012). [12] Popova, O., et al., *M&PS* 36, 905-925 (2003). [13] Holsapple, K.A., and Housen K.R., *Icarus* 191(2:Supplement), 586-597 (2007). [14] Lammer, H., et al.s, *Space. Sci. Rev.* 174, 113-154 (2013). [15] Manning, C.V., et al. *Icarus* 180, 38-59 (2006). [16] Manga, M., et al., *GRL* 39, L01202, doi:10.1029/2011GL050192 (2012). [17] Vasavada, A.R., et al., *JGR* 98, 3469-3476 (1993). [18] Kite, E.S., et al., *Icarus* 225, 850-855 (2013). [19] Dundas, C.M., et al., *GRL* 37, L12203 (2010). [20] Holsapple, K.A., *AREPS* 21, 333-373 (1993). [21] van Berk, W., et al., *JGR* 117, E10008 (2012). [22] Brown P., et al., *Nature* 420, 294-296 (2002). [23] Davis, P., *Icarus* 105, 469-478 (1993). [24] Ceplecha, Z., et al., *Space Sci. Rev.* 84, 327-341 (1998). [25] Cassata, W. et al., *EPSL* 221, 461-465 (2012). [26] Daubar, I.J., et al., *Icarus* 225, 506-516 (2013).